Joule Cell²ress

COMMENTARY

How to Accurately Report Transparent Luminescent Solar Concentrators

Chenchen Yang,^{1,4} Dianyi Liu,^{1,2,4} and Richard R. Lunt^{1,3,*}

Chenchen Yang joined the materials science program at Michigan State University in 2015 to work under Prof. Lunt in the Molecular and Organic Excitonics Lab. He earned his B.E. from the University of Electronic Science and Technology of China in 2012. Then he obtained his M.S. from the University of Florida in 2015. His current research focuses on transparent solar cell synthesis, fabrication, and characterization.

Dianyi Liu obtained his Ph.D. in inorganic chemistry from Lanzhou University in 2009. He then worked as a postdoc at Peking University, the University of Saskatchewan, and Michigan State University. He began as an assistant professor at Westlake University in January 2019. His research interests include flexible electronics, optoelectronic materials, and devices.

Richard R. Lunt is the Johansen Crosby Endowed Professor at Michigan State University in the Departments of Chemical Engineering & Materials Science and Physics. He earned his B.S. from the University of Delaware and his Ph.D. from Princeton University. He then worked as a post-doctoral researcher at MIT. His group focuses on understanding and exploiting excitonic photophysics and molecular crystal growth to develop unique thin-film optoelectronic devices. He is known for his pioneering

work on transparent solar cells and concentrators.

Introduction

Highly transparent solar cells and transparent photovoltaics (TPVs) can effectively harvest the incident solar energy from the surfaces of architectures, automobiles, and mobile electronics without affecting their current functionality. The primary applications of TPVs include windows, greenhouses, displays, signage, and automobiles. Therefore, aesthetic quality is just as important as photovoltaic performance, if not more. The practical strategy for TPV development is to maintain high average visible transmission (AVT > 50%) while improving the power conversion efficiency (PCE) toward the Shockley-Queisser (SQ) limit.¹

High AVT requires the entire device architecture (including the substrate, active layers, and any electrodes) to be visibly transparent, which is challenging for thin-film photovoltaic (PV) technologies. Alternatively, luminescent solar concentrators (LSCs) offer a promising approach to maximize PCE and AVT simultaneously by shifting the solar energy conversion optically to the waveguide edges through photoluminescence (PL) that is waveguided by total internal reflection.2 Without the presence of electrodes over the solar collection area, the structural simplicity enables LSCs to achieve the highest possible transparency without the need for additional patterning. Transparent luminescent solar concentrators (TLSCs) are fabricated by embedding ultraviolet (UV), or near-infrared (NIR) wavelength-selective harvesting luminophores into (or onto) the waveguide and tuning their corresponding PL into NIR so that absorption and emission reside in the invisible spectrum to maximize aesthetic quality and transparency.³ Utilizing this approach, efficiency limits of 6.9% and 20.6% are achievable for UV-only and UV- and NIR-selective TLSCs, respectively.³

Although LSC, TLSC, and thin-film TPV technologies (outlined in our companion article⁴) share some similarities in the methods for device characterization, LSC characterization is filled with a greater range of possible measurement errors. The purpose of this work is to demonstrate standardized LSC characterization protocols by comparatively measuring the key performance parameters in both correct and erroneous approaches. We outline simplifications of the device measurements that can be applied, while yielding reliable results. Common mistakes in the measurements are pinpointed with analysis of possible causes that can inflate performance. Parameters to evaluate the visible (VIS) transparency and aesthetic quality of LSC and TLSC devices are given with several examples. Finally, validation and consistency checks from independent experimental measurements are illustrated, which should be included in future LSC reports.

J-V Characterization

One of the key performance parameters for any photovoltaic device is *PCE*. The overall *PCE* of an LSC system is the product of the two component efficiencies³:

$$\eta_{LSC} = \eta_{Opt}^* \cdot \eta_{PV}^* = \frac{J_{SC} \cdot V_{OC} \cdot FF}{P_0},$$
 (Equation 1)

where η_{PV}^* is the efficiency of the edgemounted PV cell under the downshifted flux of the luminophore and η_{Opt}^* is the overall optical efficiency (see the detailed definitions of η_{PV}^* and η_{Opt}^* in Note S1). The two component efficiencies η_{PV}^* and η_{Opt}^* are helpful to understand the working principle



Joule CellPress

of the LSC system. However, we emphasize that any LSC or TLSC system should be treated the same as any other photovoltaic device; reporting only the overall optical efficiency (η_{Opt}^*) or optical efficiency at a specific wavelength $(\eta_{Opt}(\lambda))$ is not a sufficiently reliable way to represent the PCE of an LSC system (η_{LSC}) as we explain below. The best approach to acquire η_{LSC} is directly from current density-voltage (J-V) characteristics with connections made to edge-mounted PVs (in series or parallel) under standard illumination AM 1.5G.^{5,6} In *J-V* characteristic, J_{SC} is the short-circuit current density, V_{OC} is the open-circuit voltage, FF is the fill factor, and P_0 is the integrated solar power density (in Wm⁻²nm⁻¹) (i.e., AM 1.5G energy flux as the standard input). Since the area receiving incident power is the front surface of the waveguide, the measured short-circuit current density (J_{SC}) should always be divided by the area of the waveguide front surface rather than the area of the edge-mounted PV cells (a common mistake in J_{SC} and η_{LSC} calculations for LSCs).

In real-world applications, all four edges would typically be mounted with PV cells to maximize the output electrical power. For research purposes, an appropriate simplification (due to the symmetry) is to mount two edges with PV cells in parallel to make the configuration less complicated, simplify the wiring connections, and make the system less susceptible to losses from current matching cells that can stem from PV cell-to-cell variability and cell dimension variations. In this case, the other two edges should be painted black to prevent any reflection from inside or outside the waveguide. It is also acceptable to mount one edge with a PV cell with the remaining three painted black. The overall η_{LSC} can then be corrected by multiplying the current density by 2 or 4 for these two scenarios (no correction is needed for 4 edge-mounted cells, see Note S2).

Figure 1A illustrates both appropriate and erroneous ways to conduct J-V measurements. Most LSC devices are also intrinsically bifacial, which allows illumination from both sides. Therefore, light scattering or reflection behind the tested device can contribute to the total light absorption. It is necessary to place a matte black backdrop behind the tested LSC to eliminate the double-pass of light. As noted in our companion article for TPV,4 nearly 30% overestimation of the J_{SC} can be made with reflective or scattering backdrop, but this can be even greater for LSC since scattering from any reflective backdrop can result in direct illumination of the edge-mounted PV. For any LSC system, the electrical characterization should only account for the contribution from the downshifted PL. As shown in Figure 1A, if the edgemounted PVs are directly illuminated by an imperfectly collimated incident light, the overestimation of η_{LSC} (mainly from overestimated J_{SC}) can be substantial. Therefore, an opaque mask with well-defined area value should be closely placed in front of the LSC system to block any direct illumination. Such direct illumination not only leads to overestimation of the η_{ISC} but does so preferentially at smaller device areas so that the performance will not be representative of the scaling to larger-area devices. To illustrate the direct illumination effect on J-V measurements, a NIR-selective harvesting TLSC (waveguide length [L] = 50.8 mm, front active area = 25.8 cm^2) is edge-mounted with 1, 2, and 4 Si-PV cells (each PV cell has dimensions of 50.8 mm by 6.35 mm) as outlined above (detailed layouts are illustrated in Note S2). Index matching gel (or glue) is applied to couple the PV cells to the waveguide edges to reduce flux loss between the waveguide edge and the PV cells. The remaining unmounted edges are painted black to block the inlet and reflection of light. The raw current density curves are multiplied by 4, 2, and 1 as a correction,

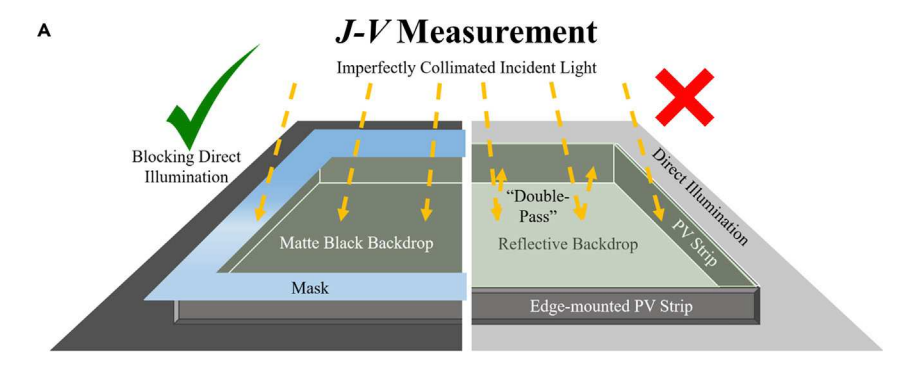
when mounting 1, 2, and 4 PV cells, respectively. The corresponding results are plotted in Figure 2A with parameters tabulated in Note S2. The slight variation in *J-V* between 1, 2, and 4 edge-mounted PVs (with masking) stems from slight variability in the PV cells and the impact of slight differences in the wiring on the *FF*. The unmasked current densities can be more than 40% higher than the ones from the masked scans, despite similar V_{OC} and *FF* values, resulting in dramatic *PCE* overestimation.

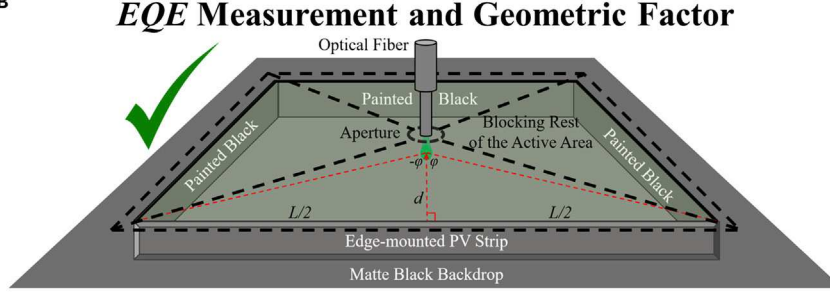
EQE_{LSC} Measurement and Matching Integrated J_{SC}

As with any other PV measurement, it is typically necessary to measure external quantum efficiency (EQE) first, to be able to measure mismatch factors and set lamp intensities appropriately prior to the measurement. This is the case for any solar cell or concentrator device that is certified. While the mismatch can be applied after the measurement to correct the illumination intensity, it is preferable to apply it first. Additionally, the comparison of the photocurrent densities extracted from J-V characteristics and integrated from EQE is the most important consistency check for any photovoltaic device. 3,4,7-9 Thus, EQE spectra should be provided in all LSC reports despite the fact that many articles fail to report such data.

For EQE measurements of LSC systems ($EQE_{LSC}(\lambda)$), several key nuances should be noted. The most reliable way to measure $EQE_{LSC}(\lambda)$ is to mount all four edges with the same PV cells (material, size, etc.) in parallel and take multiple scans at symmetrical positions all over the waveguide active area so that the average of the EQE spectrum can represent the whole waveguide for photocurrent integration (see Note S2 for details). An example of this approach is plotted as an orange curve in Figure 2B. However, to avoid unnecessarily complicated wire connections by

Joule Cell^Press





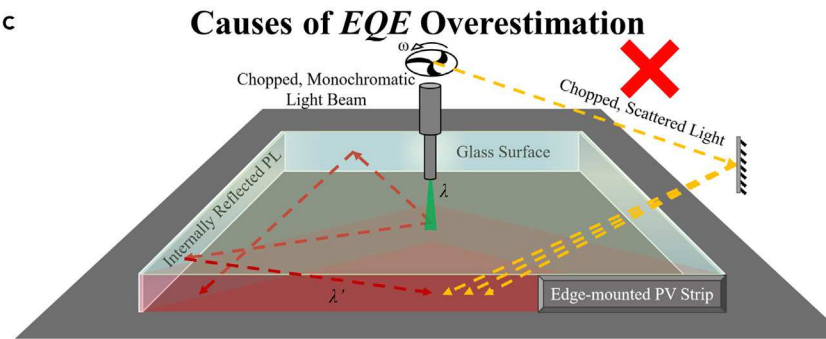


Figure 1. Schematic Protocols for LSC Characterization

(A) Schematic illustrating how to measure the J-V characteristic of LSC systems. A matte black backdrop and an opaque mask are necessary to avoid photocurrent overestimation from "double-pass" and "direct illumination" effects.

(B) Schematic showing the correct setup and the geometric factor for position-dependent EQE measurement. Note that only the incident beam is illuminated onto the front surface of the LSC waveguide, while the rest of the active area is masked. Three edges should be painted black to apply geometric correction ($\times g$ at each d) when only one edge is mounted with PV cell. (C) Schematic showing the possible causes of EQE_{LSC} overestimation. Without masking, the edge-mounted PV can pick up signal from chopped light scattered by the test environment (yellow, dashed arrows) and internal reflected PL from any unpainted edges (red, dashed arrows), causing inflated EQE_{LSC} data. Note that the edge-mounted PV should extend across the entire length of the LSC but has been shortened in the schematic for clarity.

mounting all four edges with PV cells in parallel, Figure 1B shows a simplified alternative to effectively measure EQE by mounting one edge with a PV cell and painting the rest of the three edges black. Multiple raw EQE scans are taken at various distances between the excitation beam and edge-mounted

PV cell (*d*) along the centerline. Then the $EQE_{LSC}(\lambda)$ at each *d* is calculated by multiplying the raw spectral data by the geometric factor (*g*)^{10,11}:

$$g = \frac{2\pi}{2\phi} = \frac{\pi}{\tan^{-1}\left(\frac{L}{2d}\right)},$$
 (Equation 2)

where 2ϕ is the angle facing the edgemounted PV and L is the length of the waveguide (Figures 1B and S2). This correction is only applicable along the centerline and when the other edges are painted black. An evenly spaced series of corrected measurements can then be averaged into one $EQE_{LSC}(\lambda)$ spectrum to represent the whole LSC device, which can be integrated with the AM 1.5G to compare with the corresponding J_{SC} extracted from J-V measurements. As an example, the averaged $EQE_{LSC}(\lambda)$ from the five EQE scans (d: 5-45 mm alone the centerline, 10 mm interval) of the same NIR-selective TLSC (with waveguide length L = 50.8 mm) is plotted in Figure 2B. The corresponding integrated J_{SC} (J_{SC}^{Int}) values at each d are shown as black spheres in Figure 2D. The J_{SC}^{Int} matches the J_{SC} from J-V measurement with masking. With the same TLSC, Figure 2B also illustrates that the 1 and 4 edge-mounted PVs are equivalent to each other (note the black and orange solid stars in Figures 2A and 2B; see Note S2).

Several common errors in EQE measurements can be directly identified from the spectrum. For example, nano-particles may be generated in the fabrication process. These nanoparticles function as Rayleigh scattering centers within the LSC waveguide. While scattering increases the light harvesting for small device sizes, it creates two detrimental effects: (1) haze, which is unacceptable in many applications, and (2) increased outcoupling of waveguided light that results in outcoupling loss that dominates performance as devices increase in size beyond several centimeters. To highlight the presence of such an effect, we purposely introduce nanoparticles into a NIR-selective TLSC in Figure 2C. Rayleigh scattering decreases as wavelength increases, which is reflected in the EQE spectrum as an inclined "background" superimposed to the EQE of the luminophores (blue

Joule Cell²ress

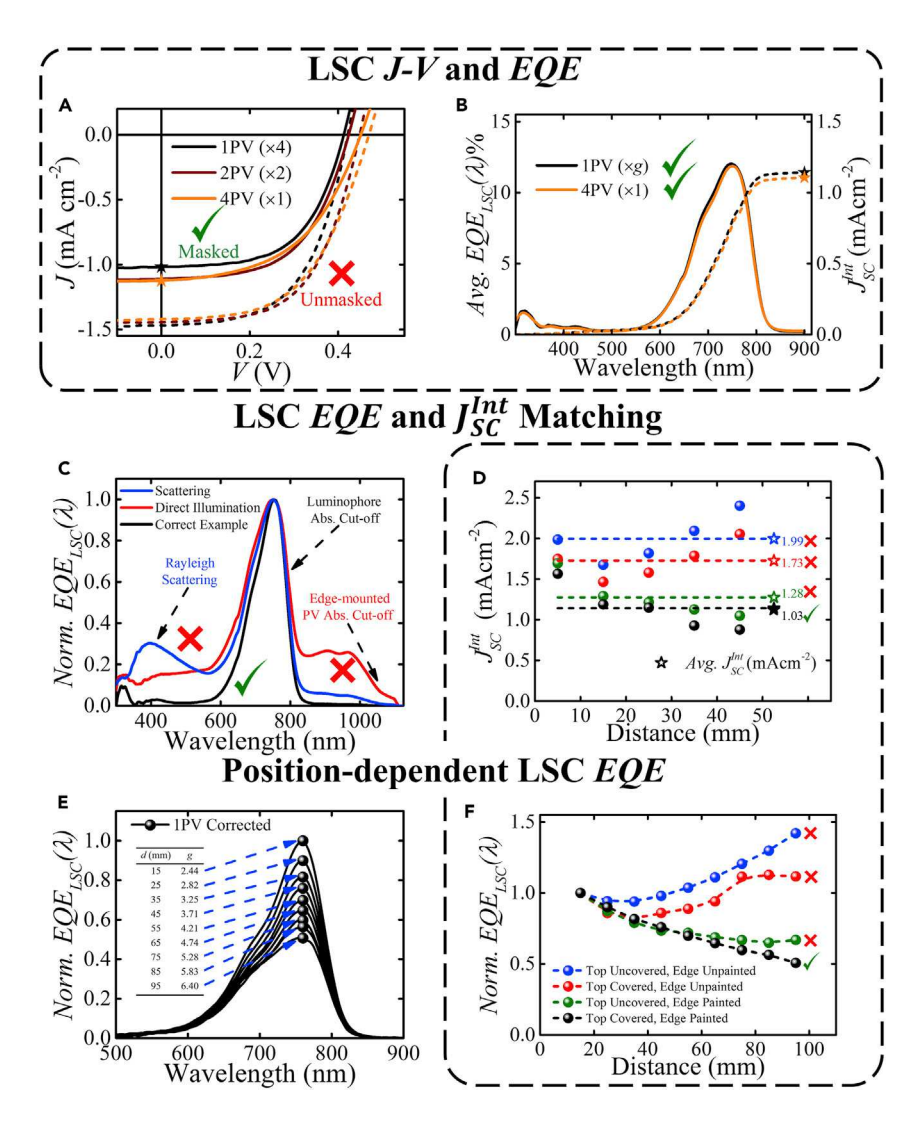


Figure 2. LSC Photovoltaic Performance

(A) J-V comparison of the same NIR-selective harvesting TLSC using different numbers of edgemounted PV strips (wired in parallel) with and without applying a mask. J-V data are measured under simulated AM 1.5G solar illumination (xenon arc lamp with the spectral mismatch factor of 0.97 \pm 0.03). Following the recommended protocols, the number of PV cells used should not significantly affect the result by more than 5%–10%.

(B) Comparison of $EQE_{LSC}(\lambda)$ spectra acquired from 1 (5 points along the centerline, corrected by x g, then averaged) and 4 edge-mounted PV cells (averaged from 13 symmetrical positions on the waveguide with no correction). Both of the corresponding J_{SC}^{int} match the J_{SC} extracted from J-V characteristics with matte black backdrop and mask shown in (A).

(C) Common errors can be directly seen in EQE measurement including scattering (sloped background) and direct illumination of the PV cell (additional offset with the PV bandgap cutoff visible).

(D) J_{SC}^{int} from $EQE_{LSC}(\lambda)$ at different positions (d: 5–45 mm with 10 mm interval, corrected by $\times g$, as spheres) and the corresponding averaged J_{SC}^{int} (dashed lines pointing the stars). Various appropriate and inappropriate scenarios are included: blue (waveguide front surface uncovered and edges unpainted), red (waveguide front surface covered and edges unpainted), olive (waveguide front surface uncovered and edges painted), and black (waveguide front surface covered and edges painted, the only correct scenario). Note the severity of "internally reflected PL" effect originates from unpainted edges, "chopped and scattered light" effect originates from uncovered waveguide front surface, and both combined can affect the $EQE_{LSC}(\lambda)$ for J_{SC}^{int} calculation.

Figure 2. Continued

(E) An example of using normalized position-dependent $EQE_{LSC}(\lambda)$ spectra (corrected by $\times g$) to predict the scalability of a NIR-selective harvesting TLSC. Inset: geometric correction factor (g) for different d values.

(F) The "internally reflected PL" and "chopped and scattered light" effects combined can affect the roll-off behavior (scalability prediction) in normalized position-dependent $EQE_{LSC}(\lambda)$ measurements.

(D) and (F) share the same legends. Data in the dashed-line boxes are encouraged to be provided in all LSC reports.

curve). If the excitation beam is not well focused and instead diverges (most optical fibers), the PV cell can be directly illuminated by the monochromatic excitation. In this case, a level background will also appear in the EQE spectrum (red curve in Figure 2C) that extends to the absorption cut-off of the edge-mounted PV. Therefore, the integrated J_{SC} will be significantly overestimated.

Position-Dependent *EQE* for Reabsorption Loss Analysis

The wavelength-dependent EQE spectrum of an LSC system ($EQE_{LSC}(\lambda)$) can be expressed as:

$$\begin{split} EQE_{LSC}(\lambda) &= \eta_{Opt}(\lambda) \bullet \\ & \frac{\int EQE_{PV}(\lambda')PL(\lambda')d\lambda'}{\int PL(\lambda')d\lambda'}, \\ & \frac{\int PL(\lambda')d\lambda'}{\int PL(\lambda')d\lambda'}, \end{split}$$
 (Equation 3)

where $\eta_{\mathit{Opt}}(\lambda)$ is the position-dependent LSC optical efficiency, which is defined as the ratio of the number of emitted photons waveguided to the edge to the number of photons incident onto the front active area at the absorption wavelength of the luminophore (λ). The integral term represents the EQE of the edgemounted PV cell over the emission wavelengths of the luminophore, and $PL(\lambda')$ is the luminophore photoluminescence emission spectrum in waveguide matrix as a function of wavelength. If the edge-mounted PV shows a nearly constant $EQE_{PV}(\lambda^{'})$ in the λ' range, Equation 3 simplifies to

Joule Cell²ress

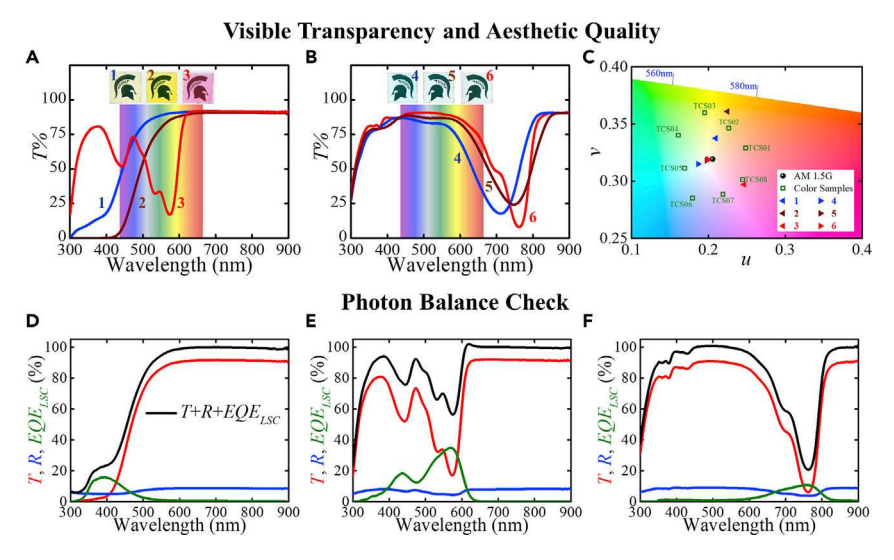


Figure 3. Aesthetic Quality and Photon Balance

(A and B) Transmission spectra of various (A) UV- and VIS- (1–3) and (B) NIR-selective (4–6) harvesting LSC and TLSCs. Inset: images of the corresponding LSC and TLSC devices photographed in transmission mode.

(C) CIE 1960 color space used to calculate *CRI* with test color samples (TCS01 to TCS08) and LSC and TLSC devices 1–6. AM 1.5G is also included as the "reference light source" point. (D–F) Photon balance check for (D) UV-, (E) VIS-, and (F) NIR-selective harvesting LSC and TLSC device examples.

 $EQE_{LSC}(\lambda) = \eta_{Opt}(\lambda) \cdot EQE_{PV}$. Then the position-dependent $EQE_{LSC}(\lambda)$ is proportional to $\eta_{Opt}(\lambda)$, which can be used to calculate the optical efficiency and predict the scalability of LSC systems. As an example, the normalized $EQE_{LSC}(\lambda)$ of a NIR-selective TLSC ($L=101.6\,$ mm) spectra as a function of d (from 15 mm to 95 mm along the centerline, with 10 mm interval) are plotted in Figure 2E, and the peak values are extracted and plotted in Figure 2F to emphasize the "roll-off" or reabsorption loss behavior.

As shown in Figure 1B, we emphasize that it is important to: (1) keep the fiber close and perpendicular to the LSC front surface, which can minimize the diverge of the excitation beam; (2) blacken the rest of the three edges, which eliminates any incident light from outside and PL reflection from inside of the waveguide edges; and (3) mask the active area while leaving a small aperture to allow the excitation into the waveguide, which prevents the edge-mounted PV from collecting

chopped and scattered light from the testing environment. Correct $EQE_{LSC}(\lambda)$ measurements should only allow the down-shifted PL signal to be collected by the edge-mounted PV cell. Due to the amplification of the correction applied (g) when using the simplified approaches, ignoring such detail can lead to severe overestimation of the J_{SC}^{Int} and incorrect roll-off behavior of the $EQE_{LSC}(\lambda)$, which are plotted in Figures 2D and 2F for comparison. For a fair comparison, we encourage J-V, averaged $EQE_{LSC}(\lambda)$, matched J_{SC}^{Int} , and $EQE_{LSC}(\lambda)$ as a function of d to be provided in all LSC reports, which are highlighted in the dashed-line box in Figure 2.

Figures of Merit for Aesthetic Quality

Aesthetic quality is equally important as *PCE* since it determines the threshold for TLSCs to be deployed in practical applications (e.g., glazing systems, mobile surfaces, etc.). *AVT*, color rendering index (*CRI*), and CIELAB color coordinates (*a**, *b**) are the three

main figures of merit to quantitatively evaluate aesthetic quality of a TLSC device. AVT is used to evaluate the overall visible transparency of a TLSC device, and CRI (with a^* , b^*) is to quantify the rendered color fidelity of the transmitted light. Standard protocols to measure and calculate these key parameters are outlined in our companion article.4 Several UV-, VIS-, and NIR-selective harvesting LSC and TLSCs are provided as examples for aesthetic quality analysis as shown in Figures 3A-3C (see Note S3; a spreadsheet is provided to calculate these parameters based on input transmittance or reflectance spectra in our companion article⁴).

Measurement Validation, Data Completeness, and Self-Consistency

Analogous to TPVs, the photon balance at every wavelength should also be satisfied for LSC systems with independent measurements of $EQE_{LSC}(\lambda)$, $T(\lambda)$, and $R(\lambda)^4$:

$$EQE_{LSC}(\lambda) / m + R(\lambda) + T(\lambda) \le 1,$$
 (Equation 4)

where m is the number of emitted photons per absorbed photon. This relation is valid since $EQE_{LSC}(\lambda)/m \le A(\lambda)$, where $A(\lambda)$ is the absolute absorption spectra of the LSC. For down-shifting luminophores, there is only one emitted photon per absorbed photon (m = 1). For downconverting luminophores that exhibit multiple exciton generation (MEG),¹² quantum-cutting (QC), 13 or singlet fission (SQ),¹⁴ the luminophore can emit more than one photon (m > 1) per absorbed photon. If these luminophores also exhibit high PL quantum yield (QY > 100%), the $EQE_{LSC}(\lambda)$ of the corresponding LSC systems can exhibit $EQE_{LSC}(\lambda) > 100\%$ at absorption peak wavelengths. Equation 4 is still valid for cases with m > 1 since $EQE_{LSC}(\lambda)/m$ is $\leq A(\lambda)$. Examples of this consistency check are shown for UV-, VIS-, and NIR-selective harvesting LSC and TLSC in Figures 3D, 3E, and 3F, respectively.

Joule CellPress

We note that the highest $EQE_{LSC}(\lambda)$ (acquired at the smallest d value) in the position-dependent EQE spectra should be used in Equation 4 to ensure the whole EQE series can satisfy the photon balance.

Conclusion

Luminescent solar concentrators provide a compelling alternative to PVs and TPVs due to their structural simplicity, low cost, high defect tolerance, and selective harvesting tunability. However, there has been substantial confusion about the best practices for characterization and performance reporting. Fundamentally, LSCs are photovoltaic systems and should therefore provide similar reporting metrics including PCE and EQE. In this work, standard protocols to characterize the performance of LSCs are provided with a particular emphasis on the simplification and challenges of performing J-V and EQE measurements. Key parameters to evaluate the visible transparency and aesthetic quality of LSC devices are outlined by using several TLSC examples. In addition, methods for confirming the self-consistency of LSC data are described. We reemphasize that all reports on LSCs should provide independent measurements of PCE, $EQE_{LSC}(\lambda)$, $T(\lambda)$, $R(\lambda)$, and QY for data completeness and show self-consistency checks to minimize potential experimental errors. In addition, AVT, light utilization efficiency (LUE), and (a*, b*) should be reported to so that aesthetics can be quantitatively compared. We expect the standardization of reporting LSC devices will ultimately help these devices advance in a sustainable, reliable, and repeatable way.

SUPPLEMENTAL INFORMATION

Supplemental Information can be found online at https://doi.org/10.1016/j.joule.2019.10.009.

ACKNOWLEDGMENTS

The authors gratefully acknowledge support from the National Science

Foundation under grant CBET-1702591. The authors also thank Scott Bankroff from MSU Department of Chemistry for preparing glass samples for this work.

DECLARATION OF INTERESTS

R.R.L. is a founder and minority shareholder of Ubiquitous Energy Inc., a company working to commercialize transparent solar cells.

- Traverse, C.J., Pandey, R., Barr, M.C., and Lunt, R.R. (2017). Emergence of highly transparent photovoltaics for distributed applications. Nat. Energy 2, 849–860.
- Debije, M.G., and Verbunt, P.P.C. (2012). Thirty Years of Luminescent Solar Concentrator Research: Solar Energy for the Built Environment. Adv. Energy Mater. 2, 12–35.
- Yang, C., and Lunt, R.R. (2017). Limits of Visibly Transparent Luminescent Solar Concentrators. Adv. Opt. Mater. 5, 1600851.
- 4. Yang, C., Liu, D., Bates, M., Barr, M.C., and Lunt, R.R. (2019). How to accurately report transparent solar cells. Joule 3, 1803–1809.
- Banal, J.L., Zhang, B., Jones, D.J., Ghiggino, K.P., and Wong, W.W.H. (2017).
 Emissive Molecular Aggregates and Energy Migration in Luminescent Solar Concentrators. Acc. Chem. Res. 50, 49–57.
- 6. Bergren, M.R., Makarov, N.S., Ramasamy, K., Jackson, A., Guglielmetti, R., and McDaniel, H. (2018). High-Performance CulnS2 Quantum Dot Laminated Glass Luminescent Solar Concentrators for Windows. ACS Energy Lett. 3, 520–525.
- Snaith, H.J. (2012). How should you measure your excitonic solar cells? Energy Environ. Sci. 5, 6513–6520.
- 8. Zimmermann, E., Ehrenreich, P., Pfadler, T., Dorman, J.A., Weickert, J., and Schmidt-Mende, L. (2014). Erroneous efficiency reports harm organic solar cell research. Nat. Photonics 8. 669.
- Snaith, H.J. (2012). The perils of solar cell efficiency measurements. Nat. Photonics 6, 337.
- Currie, M.J., Mapel, J.K., Heidel, T.D., Goffri, S., and Baldo, M.A. (2008). High-efficiency organic solar concentrators for photovoltaics. Science 321, 226–228.
- Batchelder, J.S., Zewail, A.H., and Cole, T. (1981). Luminescent solar concentrators. 2: Experimental and theoretical analysis of their possible efficiencies. Appl. Opt. 20, 3733–3754.
- Nozik, A.J. (2008). Multiple exciton generation in semiconductor quantum dots. Chem. Phys. Lett. 457, 3–11.

- Luo, X., Ding, T., Liu, X., Liu, Y., and Wu, K. (2019). Quantum-Cutting Luminescent Solar Concentrators Using Ytterbium-Doped Perovskite Nanocrystals. Nano Lett. 19, 338–341.
- Nozik, A.J. (2010). Nanoscience and nanostructures for photovoltaics and solar fuels. Nano Lett. 10, 2735–2741.

¹Department of Chemical Engineering and Materials Science, Michigan State University, East Lansing, MI 48824, USA

²School of Engineering, Westlake University, 18 Shilongshan Road, Hangzhou 310024, China

³Department of Physics and Astronomy, Michigan State University, East Lansing, MI 48824, USA

⁴These authors contributed equally

*Correspondence: rlunt@msu.edu

https://doi.org/10.1016/j.joule.2019.10.009

COMMENTARY

How to Measure the Reaction Performance of Heterogeneous Catalytic Reactions Reliably

Mengtao Zhang,¹ Meng Wang,¹ Bingjun Xu,^{2,*} and Ding Ma^{1,*}

Ding Ma is a professor of Peking University. He is an advisory member for various journals, has been Associate Editor for the catalysis journal of RSC, Catalysis Science & Technology, since 2014, and was elected as a Fellow of the Royal Society of Chemistry in 2016. His research interests are heterogeneous catalysis, especially those related with energy issues, including C₁ chemistry (methane, CO₂, and syngas conversion), new reaction routes for sustainable chemistry, and the development of an in situ spectroscopic method that can be operated at working reaction conditions to study reaction mecha-

Bingjun Xu is an Associate Professor in the Department of Chemical and Biomolecular Engineering at University of



JOUL, Volume 3

Supplemental Information

How to Accurately

Report Transparent

Luminescent Solar

Concentrators

Chenchen Yang, Dianyi Liu, and Richard R. Lunt

How to Accurately Report Transparent Luminescent Solar Concentrators

Chenchen Yang,^{1, *} Dianyi Liu,^{1,2 *}, Richard R. Lunt^{1,3,a)}

¹ Department of Chemical Engineering and Materials Science, Michigan State University,

East Lansing, MI, 48824 USA

²School of Engineering, Westlake University, 18 Shilongshan Road, Hangzhou, 310024
China

³ Department of Physics and Astronomy, Michigan State University, East Lansing, MI, 48824 USA

^{a)} Correspondence: <u>rlunt@msu.edu</u>

*The authors C.Y and D. L made equal contribution to the work.

Note 1 Detailed Description of Model Parameters

Several model parameters appear in the main text of this work, and their detailed descriptions are given as follow: the efficiency of the edge-mounted PV cell, η_{PV}^* , is the efficiency of the PV under the waveguided PL spectra and intensity of the luminophore. To a first approximation, it can be estimated by the efficiency of the PV at AM 1.5G normalized by its solar spectrum absorption efficiency and external quantum efficiency (EQE_{PV}) at the luminophore PL wavelength to account for photon downshifting:¹

$$\eta_{PV}^* = \left(\frac{\eta_{PV} \left(AM \ 1.5G\right)}{\eta_{Abs}^{PV} \left(AM \ 1.5G\right)}\right) \cdot \frac{\int EQE_{PV} \left(\lambda'\right) \cdot PL\left(\lambda'\right) d\lambda'}{\int PL\left(\lambda'\right) d\lambda'}$$
(S1)

where $\eta_{PV}\left(AM\ 1.5G\right)$ is the power conversion efficiency of the edge-mounted PV cell under AM 1.5G illumination, $PL\left(\lambda'\right)$ is the luminophore photoluminescence emission spectrum in waveguide matrix as a function of wavelength, and $\eta_{Abs}^{PV}\left(AM\ 1.5G\right)$ is the absorption efficiency of the PV active material (not the luminophore), which is defined as:

$$\eta_{Abs}^{PV}(AM\ 1.5G) = \frac{\int AM\ 1.5G(\lambda) \cdot A_{PV}(\lambda) d\lambda}{\int AM\ 1.5G(\lambda) d\lambda}$$
(S2)

where $A_{PV}(\lambda)$ is the absolute absorption spectrum of the PV active layer (no parasitic absorption of other layers), and AM 1.5 $G(\lambda)$ is the AM 1.5G photon flux. Equation S1 assumes that there is an equivalent photon flux at the waveguide edge as on the front surface from AM 1.5G. However, this is rarely the case - the flux is typically much lower

at the waveguide edge so that η_{PV}^* is light intensity dependent and its value will vary significantly (including the subcomponents of V_{OC} and FF) with the degree of concentration, luminophore QY, reabsorption loss etc.

The overall optical efficiency, η_{Opt}^* , is defined as the ratio of number of luminescent photons reaching the waveguide edge to the number of solar photons incident onto the waveguide front active surface across all incident wavelengths. Different from the overall optical efficiency η_{Opt}^* , $\eta_{Opt}(\lambda)$ is the optical efficiency at each specific wavelength λ , which is important for considering the quantum efficiency. From Eq. 3 and Eq. 5, $\eta_{Opt}(\lambda)$ is the product of several component efficiencies:

$$\eta_{Opt}(\lambda) = (1 - R_f(\lambda)) \cdot A(\lambda) \cdot \eta_{PL} \cdot \eta_{Trap} \cdot \eta_{RA}$$
 (S3)

where η_{Opt}^* and $\eta_{Opt}(\lambda)$ are related by:

$$\eta_{Opt}^* = \frac{\int AM \ 1.5G(\lambda) \, \eta_{Opt}(\lambda) d\lambda}{\int AM \ 1.5G(\lambda) d\lambda}$$
 (S4)

Combining Eq. S1 and S4 to Eq. 1 to derive the equation for power conversion efficiency of the LSC system (η_{LSC}):

$$\eta_{LSC} = \eta_{Opt}^* \cdot \eta_{PV}^* = \left[\eta_{PV} \left(AM \ 1.5G \right) \cdot \frac{\int AM \ 1.5G(\lambda) d\lambda}{\int AM \ 1.5G(\lambda) \cdot A_{PV}(\lambda) d\lambda} \cdot \frac{\int EQE_{PV}(\lambda') \cdot PL(\lambda') d\lambda'}{\int PL(\lambda') d\lambda'} \right] \cdot \left[\frac{\int AM \ 1.5G(\lambda) \eta_{Opt}(\lambda) d\lambda}{\int AM \ 1.5G(\lambda) d\lambda} \right]$$

which can be further simplified to:

$$\eta_{LSC} = \eta_{PV} \left(AM \ 1.5G \right) \cdot \frac{\int AM \ 1.5G(\lambda) \, \eta_{Opt}(\lambda) d\lambda}{\int AM \ 1.5G(\lambda) \cdot A_{PV}(\lambda) d\lambda} \cdot \frac{\int EQE_{PV}(\lambda') \cdot PL(\lambda') d\lambda'}{\int PL(\lambda') d\lambda'}$$
 (S5)

Equation S5 essentially takes the equation for the $\eta_{PV} = V_{OC}J_{SC}FF/P_0$ and corrects the J_{SC} to account for the downshifting and waveguiding of part of the solar spectrum by the luminophore. The derivation above is valid only if the photon flux density at the solar cell edge is the same as the front surface.

Thus, reporting only the overall optical efficiency (η_{Opt}^*) or optical efficiency at a specific wavelength ($\eta_{\mathit{Opt}} \left(\lambda \right)$) is not a sufficiently reliable way to represent the *PCE* of an LSC system (η_{LSC}). While there are a number of reports that only give the optical efficiency or calculate the $\,\eta_{{\scriptscriptstyle LSC}}\,$ based on assumptions of the edge-mounted PV $(\,\eta_{{\scriptscriptstyle PV}}^*\,),$ this often leads to misleading reports as η_{PV}^* is also often misunderstood and the performance of the edge-mounted PVs is intrinsically light-intensity dependent (and therefore lightconcentration dependent). Even with the same PV cell applied (same $\eta_{PV}(AM\ 1.5G)$), $\eta_{\scriptscriptstyle PV}^*$ can still vary for different LSC systems, since the $\eta_{\scriptscriptstyle Opt}^*$ will determine the intensity and the wavelength of the waveguide photon flux onto the edge-mounted PV. Moreover, it is not clear to many researchers whether η_{Opt}^* in Eq. 1 is defined on an energy or photon basis (typically it should be on photon basis as this is how PVs and LSCs work). This correspondingly depends on how η_{PV}^* is defined, often making comparisons between optical efficiencies very difficult. Instead of calculating $\eta_{\scriptscriptstyle PV}^*$ and $\eta_{\scriptscriptstyle Opt}^*$ with such complicated derivations from Eq. S1 to Eq. S5, the most straightforward approach to acquire η_{LSC} is directly from current density-voltage (J-V) characteristics with connections made to edge-mounted PVs (in series or parallel) under standard illumination AM 1.5G.

The definition of optical efficiency (η_{Opt}) is used in some literature based on the comparison of the short-circuit current density values collected with and without the LSC waveguide:

$$\eta_{Opt} = \frac{I_{LSC}}{I_{PV} \cdot G}, \text{ where } G = \frac{A_{LSC}}{A_{PV}}$$
(S6)

 η_{Opt} is defined as the number of photons emitted from the LSC edge over the total number of photons impinging on the LSC through the top surface. Eq. S6 can be used as an estimation. However, a particular problem that arises with this approach is the potential convolution of monochromatic and broad spectrum measurements so that this equation is just an estimation based on the assumption that EQE_{PV} and EQE_{LSC} are constant and the same at all wavelengths. Under broad spectrum illumination, this equation fails to capture the differing mismatch factors (and therefore equivalent intensities) from the light source for each current response in the ratio. Moreover, to make these measurements, a PV cell must have already been mounted around the edge so it is better to simply measure and report EQE_{LSC} , J-V, and PCE. Thus, while this method can be used as a quick estimate, we recommend instead providing the PCE and EQE.

A final consistency check for $EQE_{LSC}(\lambda)$ is to confirm that the absolute peak (maximum) value of the $EQE_{LSC}(\lambda)$ since this can be defined by the component efficiencies as

$$EQE_{LSC}(\lambda) = (1 - R_f(\lambda)) \cdot A(\lambda) \cdot \eta_{PL} \cdot \eta_{Trap} \cdot \eta_{RA} \cdot EQE_{PV}$$
 (S7)

where $R_f(\lambda)$ is the reflection spectrum of the incident light at the front surface, $A(\lambda)$ is the absolute absorption spectra of the LSC, η_{PL} is the PL quantum yield (QY of the luminophore in the waveguide matrix material), η_{Trap} is the photon trapping (or waveguiding) efficiency, η_{RA} is the efficiency of suppressing reabsorption.

Note 2 Equivalent Approaches for J-V and EQE_{LSC} Measurements

Figure S1 illustrates the equivalent layouts for J-V measurement for LSC systems. By following the protocols described in the main text and applying the corresponding corrections (\times 4 for "1PV", \times 2 for "2PV" and \times 1 for "4PV"), all three of the J-V equivalent layouts should lead to very similar photovoltaic performance.

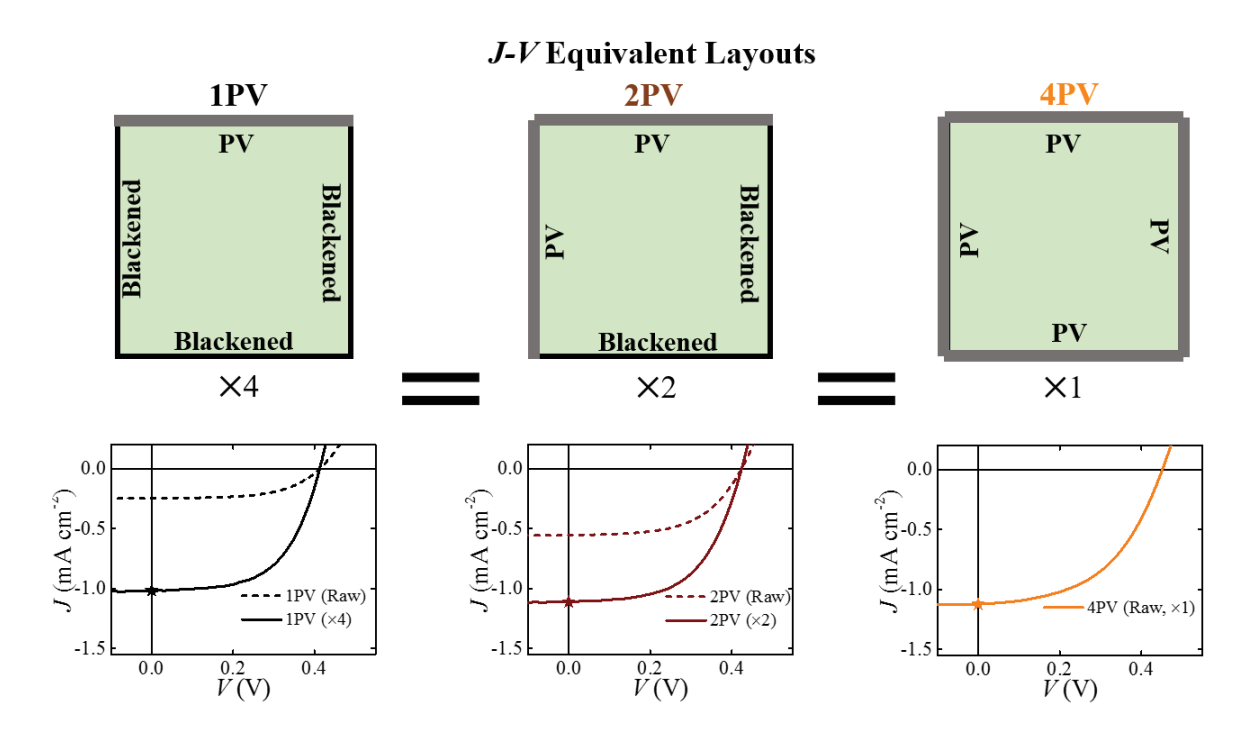


Figure S1 Equivalent layouts for *J-V* measurement for a TLSC system. Both the raw and corrected *J-V* curves are also shown in the same plot for these three layouts, respectively.

For the $EQE_{LSC}(\lambda)$ measurement example (L=50.8mm) provided in this work, we use both 1PV- and 4PV-approaches: for 1PV approach, 5 scans are taken along the center lines with 10mm interval, then each EQE spectrum is corrected by multiplying the corresponding g at each d, then these 5 corrected spectra (after $\times g$) are averaged as the representative $EQE_{LSC}(\lambda)$ for the whole TLSC; for the 4PV approach, 13 scans in total are taken in the symmetrical positions all over the waveguide front surface as shown in **Figure**

S2, 13 EQE spectra are averaged as the $EQE_{LSC}(\lambda)$ and no correction is needed in 4PV scenario. These two approaches are equivalent and result in very similar J_{SC}^{Int} values as shown in **Figure 2**B, which match the J_{SC} from 1PV, 2PV and 4PV approaches for J-V measurement.

PV Blackened Xg, Avg. Avg.

Figure S2 Equivalent layouts for EQE measurement for a TLSC system.

Table S1 summarizes the photovoltaic parameters of this TLSC. Note the difference between the conditions with and without the mask applied. The integrated short-circuit current density values (J_{SC}^{Im}) with 1 or 4 edge mounted PV cell(s) are also provided for comparison.

Approaches (XCorrection)	J _{SC} (mAcm ⁻²)	J_{SC}^{Int} (mAcm ⁻²)	<i>V_{OC}</i> (V)	FF %	PCE %
1PV Masked (X4)	1.02±0.09	1 14 () (0.41±0.01	59±1	0.24±0.02
1PV Unmasked (X4)	1.47 ± 0.08	1.14 (Xg, Avg.)	0.42 ± 0.01	57±2	0.35 ± 0.01
2PV Masked (×2)	1.11 ± 0.07	NI/A	0.42 ± 0.01	57±1	0.26 ± 0.02
2PV Unmasked (×2)	1.44 ± 0.04	N/A	0.44 ± 0.01	58±1	0.37 ± 0.02
4PV Masked (×1)	1.12 ± 0.08	1 11 (0.44 ± 0.01	51±1	0.25 ± 0.02
4PV Unmasked (X1)	1.42 ± 0.01	1.11 (Avg.)	0.46 ± 0.01	54±1	0.36 ± 0.01

Table S1 Comparison of photovoltaic parameters of the TLSC with and without mask.

Note 3 Aesthetic Quality Analysis for LSC and TLSC Examples

The absence of electrodes and complex optical interference enables both higher levels of visible transparency and color tuning for LSC and TLSCs. LSCs can be designed to be colorful (for exteriors) or invisible (for windows and displays) by tuning the absorption wavelength range of the embedded luminophores. The transmission spectrum $(T(\lambda))$ of an LSC or TLSC is the input data for its AVT, CRI and color coordinates calculation. As an example, **Figure 3**A and B show $T(\lambda)$ of several LSC and TLSC systems embedded with various luminophores (1 to 2 for UV-, 3 for VIS-, 4 to 6 for NIR-selective harvesting).

Table 2 Summary of aesthetic quality parameters of various samples.

Samples	AVT%	CRI	CIELAB (a^*, b^*)
AM 1.5G	100	100	(0, 0)
UV-TLSC-1	87.7	90.8	(-5.8, 25.2)
UV-TLSC-2	77.8	69.9	(-5.1, 68.7)
VIS-LSC-3	43.6	27.7	(33.3, -17.9)
NIR-TLSC-4	76.6	77.4	(-12.4, -6.9)
NIR-TLSC-5	84.5	90.3	(-5.3, -2.2)
NIR-TLSC-6	87.9	92.8	(-4.9, -0.9)

By applying a series of mathematical transformation, $T(\lambda)$ can be converted into (u, v) coordinates in CIE 1960 uniform color space (CIELUV) as shown in Figure 3C, where the chromaticity coordinate distance between the point of the reference AM 1.5G and the point of the transmitted source determines the chromaticity difference and the corresponding CRI. Alternatively, the input $T(\lambda)$ can also be converted into (a^*, b^*) coordinates as the report

of color rendering property as tabulated in **Table S2**. As the selective harvesting cut-offs blue-shift into UV (from device 3 to 1 in Figure 3A) or as the selective harvesting peaks red-shift from into NIR (from device 4 to 6 in Figure 2B), the corresponding AVT and CRI increase, and the (u, v) coordinates approach the AM 1.5G reference source point. The inset photographs of the LSC and TLSCs concomitantly agree with such trend: the observed colors change from pinkish to light-yellow from device 3 to 1 and from light-blue to nearly colorless from device 4 to 6. Therefore, these figures of merit should be reported in the future LSC works as long as aesthetics are considered as their properties. A spreadsheet is provided in our companion article to calculate all the aesthetic parameters based on an input $T(\lambda)$ or $R(\lambda)$ spectra.²

Note 4 Experimental Section

Module Fabrication:

- 1) UV-Selective harvesting TLSCs: Cs₂Mo₆I₈(CF3CF2COO)₆ nanocluster³ for UV-TLSC-1 and UV-TLSC-2 was dissolved in ethanol to prepare the solution. The ethanol solution was mixed with mounting medium (Fluoroshield F6182, Sigma-Aldrich) at a volume ratio of 1:2.
- 2) VIS-Selective harvesting LSC: Lumogen F Red 305 (BASF) for VIS-LSC-3 was dissolved in dichloromethane to prepare the solution. The dichloromethane solution was mixed with (poly)-butyl methacrylate-co-methyl methacrylate (PBMMA, Sigma-Aldrich) at a volume ratio of 1:1.
- 3) NIR Selective harvesting TLSCs: Cy7-NHS (Lumiprobe) for NIR-TLSC-6 (Cy7-NEt₂-I⁴ for NIR-TLSC-4 and Cy7.5-NEt₂-I⁴ for NIR-TLSC-5) powder was dissolved in ethanol to prepare the solution. The ethanol solution was mixed with mounting medium (Fluoroshield F6182, Sigma-Aldrich) at a volume ratio of 1:2.

This mixture was drop-cast on 50.8mm \times 50.8mm \times 6.35mm (for J-V characterization and averaged EQE_{LSC} measurement (Figure 2A to D)) and 101.6mm \times 101.6mm \times 6.35mm (for position-dependent EQE_{LSC} (Figure 2E and F)) glass sheets and allowed to dry for 6h in a glove-box filled with nitrogen gas (O₂, H₂O < 1ppm). Single crystalline solar cells (Vikocell Solar) were laser-diced in to 50.8mm \times 6.35mm strips for J-V characterization and averaged EQE_{LSC} measurements, and 101.6mm \times 6.35mm strips for position-dependent EQE_{LSC} measurements. Index matching gel (Thorlabs) was used to attach the PV cells onto

the edge of the waveguides. The unmounted edges were painted black to block the light and internal reflection of PL.

Optical Characterization: Specular transmittance $(T(\lambda))$ of both solutions and TLSC devices were measured using a double-beam Lambda 800 UV/VIS spectrometer in the transmission mode. No reference sample was placed on the reference beam side for TLSC transmittance measurement. Reflectance $(R(\lambda))$ of the TLSCs was also measured using Lambda 800 UV/VIS spectrometer with the specular accessory installed on the sample beam side. The absorption spectra were acquired by following the equation: $A(\lambda) = 1 - T(\lambda) - R(\lambda)$.

Module Photovoltaic Characterization: A Keithley 2420 SourceMeter was used to obtain *J-V* characteristics under simulated AM 1.5G solar illumination (xenon arc lamp combined with a calculated spectra mismatch factor of 1.05 for all the TLSCs tested). The light intensity was calibrated with an NREL-calibrated Si reference diode with KG5 filter. The position-dependent *EQE_{LSC}* measurements were performed using a QTH lamp with a calibrated Si detector, monochromator, chopper and lock-in amplifier. The detailed methods and structure layouts (1PV, 2PV and 4PV for *J-V*, 1PV and 4PV for *EQE_{LSC}*) are provided in the main text and Supplemental Information Note 2. A matte black background was placed on the back of the TLSC device to eliminate illumination from the environment or reflection (double-pass) for both *J-V* and *EQE* measurements. All the TLSC devices were tested with the same Si cells to eliminate any PV-to-PV variation in performance.

Reference

- 1. Yang, C., and Lunt, R.R. (2017). Limits of Visibly Transparent Luminescent Solar Concentrators. Adv. Opt. Mater. 5, 1600851.
- 2. Yang, C., Liu, D., Bates, M., Barr, M.C., and Lunt, R.R. (2019). How to Accurately Report Transparent Solar Cells. Joule .
- Kuttipillai, P.S., Yang, C., Chen, P., Wang, L., Bates, M., Lunt, S.Y., and Lunt, R.R.
 (2018). Enhanced Electroluminescence Efficiency in Metal Halide Nanocluster
 Based Light Emitting Diodes through Apical Halide Exchange. ACS Appl. Energy
 Mater. 1, 3587–3592.
- 4. Yang, C., Zhang, J., Peng, W.-T., Sheng, W., Liu, D., Kuttipillai, P.S., Young, M., Donahue, M.R., Levine, B.G., Borhan, B., and Lunt, R.R. (2018). Impact of Stokes Shift on the Performance of Near-Infrared Harvesting Transparent Luminescent Solar Concentrators. Sci. Rep. 8, 16359.